Structure and Magnetic Properties of One-Dimensional $PPh_4[Ni(pn)_2][M(CN)_6]\cdot H_2O$ (M = Fe, Cr, Co) Bimetallic Assemblies

Masaaki Ohba,* Naoki Usuki, Nobuo Fukita, and Hisashi Ōkawa*

Department of Chemistry, Faculty of Science, Kyushu University, Hakozaki, Higashi-ku, Fukuoka 812, Japan

Received April 24, 1997

Three bimetallic assemblies, $PPh_4[Ni(pn)_2][M(CN)_6]\cdot H_2O$ (M = Fe (**1**), Cr (**2**), Co (**3**); pn = *rac*-1,2-diaminopropane), have been prepared and structurally and magnetically characterized. Assembly **2** crystallizes in the monoclinic system of the space group $P2/c$ (No. 13) with $a = 12.927(2)$ Å, $b = 8.454(2)$ Å, $c = 17.564(2)$ Å, $\beta = 100.15(1)°$, $V = 1889.5(6)$ Å^3, and $Z = 2$, and **3** crystallizes in the same space group with $a = 12.971(1)$ Å, $b = 8.437(1)$ Å, $c = 17.118(1)$ Å, $\beta = 99.84(1)°$, $V = 1845.7(3)$ Å^3, and $Z = 2$. The crystal structure analyses of **2** and **3** reveal a one-dimensional zigzag chain structure extending through the M−CN−Ni−NC−M linkages as previously found for **1**. Assemblies **1** and **2** show a ferromagnetic intrachain interaction based on the strict orthogonality of the magnetic orbitals between adjacent Ni^{II} and M^{III} (M = Fe, Cr) ions. Assembly **3** is essentially paramagnetic within the chain. All the assemblies show a weak antiferromagnetic interchain interaction and hence no magnetic ordering over the lattice.

Introduction

In the past few years there has been an increasing interest in metal assemblies constructed of paramagnetic complexes, with the aim to provide molecular-based magnets.[1−34] The general synthetic approach for the metal assemblies is to utilize metal complexes having coordination ability as building blocks. Hexacyanometalate ions are such building blocks which react with simple metal ions to give the so-called "Prussian blue analogs".[20−34] When coordinatively unsaturated complexes are used instead of simple metal ions, hexacyanometalate ions can adopt different bridging modes from η^1 to η^6 to form bimetallic assemblies of various network structures.[8−19] We are interested in cyanide-bridged bimetallic assemblies constructed from a hexacyanometalate ion (building block) and a four-coordinate $[Ni(L)_2]^{2+}$ (L = diamine ligand) complex (connecting block).[8−17] The use of four-coordinate nickel(II) instead of a simple metal ion significantly reduces the complexity in the network structure of the bimetallic assembly, and the magnetostructural studies of these bimetallic assemblies may serve to obtain fundamental bases for developing complex-based magnetic materials. Previously, we have reported four bimetallic assemblies of different

(1) Kahn, O. *Advances in Inorganic Chemistry*; Academic Press. Inc.: San Diego, 1995: Vol. 43, p 179.
(2) Kahn, O. In *Molecular Magnetism*; VCH: Weinheim, Germany, 1993.
(3) Miller, J. S.; Epstein, A. J. *Chem. Eng. News* **1995**, *73* (October), 30.
(4) Miller, J. S.; Epstein, A. J. *Angew. Chem., Int. Ed. Engl.* **1994**, *33*, 385.
(5) Gatteschi, D. *Adv. Mater.* **1994**, *6*, 635.
(6) Iwamura, H., Miller, J. S., Eds. Proceeding of the Conference on Chemistry & Physics of Molecular-Based Magnetic Materials. *Mol. Cryst. Liq. Cryst.* **1993**, *232*−*233*.
(7) Gatteschi, D., Kahn, O., Miller, J. S., Palacio, F., Eds. *Molecular Magnetic Material*; NATO ASI Series E 198; Kluwer Academic Publishers: Dordrecht, 1990.
(8) Ohba, M.; Maruono, N.; Ōkawa, H.; Enoki, T.; Latour, J. M. *J. Am. Chem. Soc.* **1994**, *116*, 11566.
(9) Ohba, M.; Ōkawa, H.; Ito, T.; Ohto, A. *J. Chem. Soc., Chem. Commun.* **1995**, 1545.
(10) Ōkawa, H.; Ohba, M. In *Molecule-Based Magnetic Materials: Theory, Techniques, and Applications*; Turnbull, M. M., Sugimoto, T., Thompson, L. K., Eds.; ACS Symposium Series 644; American Chemical Society: Washington, DC, 1996; p 319.
(11) Ohba, M.; Ōkawa, H. *Mol. Cryst. Liq. Cryst.* **1996**, *286*, 101.
(12) Ohba, M.; Fukita, N.; Ōkawa, H.; Hashimoto, Y. *J. Am. Chem. Soc.* **1997**, *119*, 1011.
(13) Ohba, M.; Fukita, N.; Ōkawa, H. *J. Chem. Soc., Dalton Trans.* **1997**, 1733.
(14) Miyasaka, H.; Matsumoto, N.; Ōkawa, H.; Re, N.; Gallo, E.; Floriani, C. *Angew. Chem., Int. Ed. Engl.* **1995**, *34*, 1446.
(15) Miyasaka, H.; Matsumoto, N.; Ōkawa, H.; Re, N.; Gallo, E.; Floriani, C. *J. Am. Chem. Soc.* **1996**, *118*, 981.
(16) Re, N.; Gallo, E.; Floriani, C.; Miyasaka, H.; Matsumoto, N. *Inorg. Chem.* **1996**, *35*, 5964.
(17) Re, N.; Gallo, E.; Floriani, C.; Miyasaka, H.; Matsumoto, N. *Inorg. Chem.* **1996**, *35*, 6004.
(18) S. El Fallah, M.; Rentschler, E.; Caneschi, A.; Sessoli, R.; Gatteschi, D. *Angew. Chem., Int. Ed. Engl.* **1996**, *35*, 1947.
(19) Farlay, S.; Mallah, T.; Vaissermann, J.; Bartolome, F.; Veillet, P.; Verdaguer, M. *Chem. Commun.* **1996**, 2481.
(20) Herren, F.; Fischer, P.; Ludi, A.; Hälg, W. *Inorg. Chem.* **1980**, *19*, 956.
(21) Klenze, H.; Kanellalopulos, B.; Tragester, G.; Eysel, H. H. *J. Chem. Phys.* **1980**, *72*, 5819.
(22) Griebler, W. D.; Babel, D. *D. Z. Naturforsch.* **1982**, *87B*, 832.
(23) Gadet, V.; Bujoli-Doeuff, M.; Force, L.; Verdaguer, M.; Malkhi, K. El, Deroy, A.; Besse, J. P.; Chappert, C.; Veillet, P.; Renard, J. P.; Beauvillain, P. In *Molecular Magnetic Material*; Gatteschi, D., et al., Eds. NATO ASI Series 198; Kluwer: Dordrecht, 1990; p 281.
(24) Gadet, V.; Mallah, T.; Castro, I.; Verdaguer, M. *J. Am. Chem. Soc.* **1992**, *114*, 9213.
(25) Mallah, S.; Thiebaut, S.; Verdaguer, M.; Veillet, P. *Science* **1993**, *262*, 1554.
(26) Entley, W. R.; Girolani, G. S. *Science* **1995**, *268*, 397.
(27) Entley, W. R.; Girolani, G. S. *Inorg. Chem.* **1994**, *33*, 5165.
(28) Ferlay, S.; Mallah, T.; Ouahés, R.; Veillet, P.; Verdaguer, M. *Nature* **1995**, *378*, 701.
(29) Kahn, O. *Nature* **1995**, *378*, 667.
(30) Sato, O.; Iyoda, T.; Fujishima, A.; Hashimoto, K. *Science* **1996**, *271*, 49.
(31) Verdaguer, M. *Science* **1996**, *272*, 698.
(32) Sato, O.; Iyoda, T.; Fujishima, A.; Hashimoto, K. *Science* **1996**, *272*, 704.
(33) Arrio, M.-A.; Sainctavit, P.; Moulin, C.; Mallah, T.; Verdaguer, M.; Pellegrin, E.; T. Chen, C. *J. Am. Chem. Soc.* **1996**, *118*, 6422.
(34) Dumbar, K. R.; Heintz, R. A. *Progress in Inorganic Chemistry*; John Wiley & Sons: New York, 1997; Vol. 45, p 283.

S0020-1669(97)00474-6 CCC: $15.00
Published on Web 06/03/1998

networks using $[Ni(L)_2]^{2+}$ (L = diamine ligand) as the connecting block: $PPh_4[Ni^{II}(pn)_2][Fe^{III}(CN)_6]\cdot H_2O$ with a 1-D zigzag chain structure,[10] $[Ni^{II}(en)_2]_3[M^{III}(CN)_6]_2\cdot 2H_2O$ (M = Fe, Mn, Cr, Co) with a 1-D rope−ladder structure,[8,10,13] $[Ni(L)_2]_2[Fe(CN)_6]X\cdot nH_2O$ (L = pn, 1,1-dimethylethylenediamine (1,1-dmen); $X^- = ClO_4^-$, BF_4^-, PF_6^-, etc.) with a 2-D sheet structure,[9−12] and $[Ni(N\text{-}men)_2]_3[Fe(CN)_6]_2\cdot 12H_2O$ (N-men = *N*-methylethylenediamine) with a honeycomb sheet structure.[35] These can be rationally prepared by the reaction of $[M(CN)_6]^{3-}$ and $[Ni(L)_3]^{2+}$ in their respective stoichiometries, in the absence or presence of an appropriate counterion. Detailed magnetic studies have been made for the bimetallic assemblies of the 1-D rope−ladder structure and the 2-D sheet structure, but only a preliminary magnetic study was reported for $PPh_4[Ni(pn)_2][Fe(CN)_6]\cdot H_2O$ (**1**).

In this study, analogous 1-D chain assemblies $PPh_4[Ni(pn)_2][Cr(CN)_6]\cdot H_2O$ (**2**) and $PPh_4[Ni(pn)_2][Co(CN)_6]\cdot H_2O$ (**3**) have been obtained which are isomorphous with **1**[10] based on X-ray crystallography. The cryomagnetic properties of **1**−**3** were studied in the temperature range of 4.2−290 K and discussed in view of the electronic configuration of the M^{III} ions.

Experimental Section

Physical Measurements. The elemental analyses of carbon, hydrogen, and nitrogen were obtained at the Service Center of Elemental Analysis of Kyushu University. Metal (chromium, cobalt, iron and nickel) analyses were made on a Shimadzu AA-680 atomic absorption/flame emission spectrophotometer. Infrared spectra were measured on a JASCO IR-810 spectrophotometer using KBr discs. Electronic spectra were recorded by the diffuse reflectance technique on a Shimadzu model MPS-2000 multipurpose spectrophotometer. Magnetic susceptibilities were measured by a HOXAN HSM-D SQUID susceptometer in the temperature range 4.2−100 K (applied magnetic field of 100 G) and by a Faraday balance in the temperature range 80−300 K (applied magnetic field of 3000 G). Calibrations were made with $Mn(NH_4)_2(SO_4)_2\cdot 6H_2O$ using the SQUID susceptometer and with $[Ni(en)_3]S_2O_3$ using the Faraday balance. Diamagnetic corrections were made with Pascal's constants. Effective magnetic moments were calculated using the equation $\mu_{eff} = 2.828(\chi_M T)^{1/2}$, where χ_M is the molar magnetic susceptibility corrected for the diamagnetism of the constituent atoms. The field dependence of the magnetization was measured using a Quantum Design MPMS-5S SQUID susceptometer.

Preparations. $[Ni(pn)_3]Cl_2$ was prepared using the literature method.[36] $K_3[Fe(CN)_6]$ (Wako Pure Chemical Industries, Ltd.), $K_3[Cr(CN)_6]$ (Mitsuwa Chemical Co.), $K_3[Co(CN)_6]$ (Nakalai Tesque Inc.), and PPh_4Cl (Tokyo Kasei Kogyo Co., Ltd.) were of reagent grade and used as purchased.

$PPh_4[Ni(pn)_2][Fe(CN)_6]\cdot H_2O$ (1). $[Ni(pn)_3]Cl_2$ (88 mg, 0.25 mmol) and PPh_4Cl (94 mg, 0.25 mmol) were dissolved in 20 cm^3 of water. To this solution was added an aqueous solution (10 cm^3) of $K_3[Fe(CN)_6]$ (82 mg, 0.25 mmol) at room temperature, and the resulting brown solution was allowed to stand overnight to form brown prismatic crystals. They were collected by suction filtration, washed with water, and dried in vacuo over P_2O_5. Yield: 120 mg, 62%. Found: C, 55.86; H, 5.57; N, 18.11; Fe, 6.9; Ni, 7.8. Calcd for $C_{36}H_{42}FeN_{10}NiOP$: C, 55.69; H, 5.45; N, 18.04; Fe 7.2; Ni, 7.6. IR (cm^{-1}, KBr disc): [ν_{CN}] 2130, 2110. λ_{max} (nm, reflectance): 270, 276, 308, 324, 418, 531^{sh}.

$PPh_4[Ni(pn)_2][Cr(CN)_6]\cdot H_2O$ (2). To a solution of $[Ni(pn)_3]Cl_2$ (88 mg, 0.25 mmol) and PPh_4Cl (112 mg, 0.3 mmol) in 20 cm^3 of a water−methanol (2:1) mixture was added an aqueous solution (10 cm^3) of $K_3[Cr(CN)_6]$ (81 mg, 0.25 mmol) at room temperature, and the resulting purple mixture was allowed to stand overnight to give light purple prismatic crystals. They were collected by suction filtration, washed with water, and dried in vacuo over P_2O_5. All the operations for the synthesis were carried out in the dark to avoid the decomposition of $K_3[Cr(CN)_6]$. Yield 130 mg, 67%. Found: C, 56.17; H, 5.49; N, 18.23; Cr, 6.3; Ni, 7.3. Calcd for $C_{36}H_{42}CrN_{10}NiOP$: C, 55.98; H, 5.48; N, 18.13; Cr 6.7; Ni, 7.6. IR (cm^{-1}, KBr disc): [ν_{CN}] 2150, 2130. λ_{max} (nm, reflectance): 270, 276, 316^{sh}, 382, 532.

$PPh_4[Ni(pn)_2][Co(CN)_6]\cdot H_2O$ (3). This was prepared as purple crystals in a reaction similar to that of **1**, except for the use of $K_3[Co(CN)_6]$ instead of $K_3[Fe(CN)_6]$. Yield 110 mg, 55%. Found: C, 55.63; H, 5.50; N, 18.05; Co, 7.5; Ni, 7.7. Calcd for $C_{36}H_{42}CoN_{10}NiOP$: C, 55.48; H, 5.43; N, 17.97; Co 7.6; Ni, 7.5. IR (cm^{-1}, KBr disc): [ν_{CN}] 2130, 2110. λ_{max} (nm, reflectance): 270, 277, 317, 543.

X-ray Crystallography. Single crystals of **2** and **3** were mounted on a glass fiber and coated with epoxy resin. All the crystallographic measurements were carried out on a Rigaku AFC7R diffractometer using graphite-monochromated Mo Kα radiation ($\lambda = 0.710\ 69$ Å) and a 12 kW rotating anode generator. The data were collected at 20 ± 1 °C using the $\omega-2\theta$ scan technique to a maximum 2θ value of 50.0° at a scan speed 16.0°/min (in ω). The weak reflections ($I < 10.0\sigma(I)$) were rescanned (maximum of 4 scans), and the counts were accumulated to ensure good counting statistics. Stationary background counts were recorded on each side of the reflection. The ratio of peak counting time to background counting time was 2:1. The diameter of the incident beam collimator was 1.0 mm, the crystal to detector distance was 235 mm, and the computer-controlled detector aperture was set to 9.0 × 13.0 mm (horizontal × vertical). The cell parameters of **2** and **3** were determined by 25 reflections in the 2θ ranges 29.49−30.00° and 29.56−30.00°, respectively. The octant measured was $\pm h$, $+k$, and $+l$ for both compounds. The intensities of the representative reflection were measured after every 150 reflections. Over the course of the data collection, the standards increased by 0.1% for **2** and decreased by 0.7% for **3**. A linear correction factor was applied to the data to account for this phenomenon. Intensity data were corrected for Lorentz and polarization effects.

The structures were solved by the direct method and expanded using a Fourier technique. The non-hydrogen atoms were anisotropically refined. Hydrogen atoms were included in the structure factor calculations and isotropically refined for **2** but not refined for **3**. The final cycle of the full-matrix least-squares refinement of **2** was based on 2775 observed reflections ($I > 3.00\sigma(I)$) and 314 variable parameters and converged with unweighted and weighted agreement factors of $R = \sum||F_o| - |F_c||/\sum|F_o| = 0.034$ and $R_w = [(\sum_w(||F_o| - |F_c||)^2/\sum F_o^2)]^{1/2} = 0.026$. The refinement for **3** was based on 2946 observed reflections ($I > 3.00\sigma(I)$) and 234 variable parameters and converged with $R = 0.073$ and $R_w = 0.073$. Neutral atom scattering factors were taken from Cromer and Waber.[37] Anomalous dispersion effects were included in F_{calc}; the values for $\Delta f'$ and $\Delta f''$ were those of Creagh and McAuley.[38] The values for the mass attenuation coefficients were those of Creagh and Hubbel.[39] All calculations were performed using the teXsan crystallographic software package from the Molecular Structure Corporation.[40]

In this study the structure of **1** was reexamined using a newly grown single crystal. The refinement based on 2231 observed reflections of $I > 3.00\sigma(I)$ gave better R and R_w values (0.077 and 0.067, respectively) compared with the previous analysis based on 2160 observed reflections of $I > 4.00\sigma(I)$ ($R = 0.081$ and $R_w = 0.076$).[10] The crystal parameters of **1**, **2**, and **3** are summarized in Table 1. The final positional parameters of the non-hydrogen atoms for **2** and **3** with their estimated standard deviations are listed in Tables 2 and 3, respectively.

Results and Discussion

General Properties. Each of **1**−**3** shows two sharp ν_{CN} bands at ∼2130 and ∼2110 cm^{-1}, indicating the existence of

(35) Ohba, M.; Shinzato, H.; et al. Unpublished result.
(36) Werner, A. *Z. Anorg. Chem.* **1899**, *21*, 210.
(37) Cromer, D. T.; Waber, J. T. In *International Tables for X-ray Crystallography*; The Kynoch Press: Birmingham, England, 1974; Vol. IV.
(38) Creagh, D. C.; McAuley, W. J. In *International Tables for Crystallography*; Kluwer Academic Publishers: Boston, MA, 1992; Vol. C.
(39) Creagh, D. C.; Hubbell, J. H. in *International Tables for Crystallography*; Kluwer Academic Publishers: Boston, 1992; Vol. C.
(40) *teXsan: Crystal Structure Analysis package*; Molecular Structure Corporation: The Woodlands, TX, 1985 and 1992.

Table 1. Crystal Parameters for **1**−**3**

	1 (M = Fe)	**2** (M = Cr)	**3** (M = Co)
fw	776.32	772.46	779.40
space group	*P*2/*c* (No. 13)	*P*2/*c* (No. 13)	*P*2/*c* (No. 13)
a/Å	12.958(3)	12.927(2)	12.971(1)
b/Å	8.437(3)	8.454(2)	8.437(1)
c/Å	17.250(2)	17.564(2)	17.118(1)
β/deg	99.96(1)	100.15(1)	99.84(1)
V/Å^3	1857.4(7)	1889.5(6)	1845.7(3)
Z	2	2	2
D_c/g cm^{-3}	1.388	1.358	1.402
μ (Mo Kα)/cm^{-1}	9.84	8.71	10.47
R^a	0.077	0.034	0.073
$R_w{}^b$	0.066	0.026	0.073

^{a} $R = \sum||F_o| - |F_c||/\sum|F_o|$. ^{b} $R_w = [(\sum(|F_o| - |F_c|)^2/\sum F_o^2]^{1/2}$.

Table 2. Selected Atomic Coordinates and Isotropic Thermal Parameters for **2**

atom	*x*	*y*	*z*	*B*(eq)
Ni	0	0	0	2.38(1)
Cr	0	0.33271(7)	1/4	2.23(1)
P(1)	1/2	0.0797(1)	1/4	3.18(3)
O(1)	0.8950(5)	0.4952(8)	0.5004(4)	11.0(2)
N(1)	0.0339(2)	0.0926(3)	0.1144(1)	3.27(6)
N(2)	−0.2399(2)	0.3279(3)	0.1605(2)	4.55(7)
N(3)	0.0527(2)	0.6045(4)	0.1366(2)	6.8(1)
N(4)	−0.1284(2)	0.1518(3)	−0.0243(2)	3.10(6)
N(5)	−0.1108(2)	−0.1512(4)	0.0361(2)	3.74(7)
C(1)	0.0276(2)	0.1688(3)	0.1674(1)	2.56(6)
C(2)	−0.1561(2)	0.3299(4)	0.1933(2)	2.96(7)
C(3)	0.0343(2)	0.5077(4)	0.1766(2)	3.68(7)
C(4)	−0.2238(2)	0.0596(4)	−0.0260(2)	4.23(9)
C(5)	−0.3221(3)	0.1552(5)	−0.0307(3)	4.7(1)
C(6)	−0.2065(3)	−0.0545(5)	0.0382(3)	5.2(1)

Table 3. Selected Atomic Coordinates and Isotropic Thermal Parameters for **3**

atom	*x*	*y*	*z*	*B*(eq)
Ni	0	0	0	2.23(2)
Co	0	0.3243(1)	1/4	2.10(2)
P(1)	1/2	0.0646(3)	1/4	3.01(5)
O(1)	0.8889(8)	0.490(1)	0.4996(6)	6.0(3)
N(1)	0.0317(4)	0.0939(6)	0.1183(2)	2.8(1)
N(2)	−0.2299(4)	0.3183(7)	0.1700(3)	4.0(1)
N(3)	0.0425(5)	0.5859(8)	0.1385(3)	6.3(2)
N(4)	−0.1256(3)	0.1586(5)	−0.0269(3)	2.8(1)
N(5)	−0.1130(4)	−0.1458(6)	0.0370(3)	3.3(1)
C(1)	0.0236(4)	0.1718(6)	0.1700(3)	2.1(1)
C(2)	−0.1448(5)	0.3218(7)	0.2006(3)	2.8(1)
C(3)	0.0279(5)	0.4883(7)	0.1791(3)	3.2(1)
C(4)	−0.2213(5)	0.0672(8)	−0.0287(4)	4.1(2)
C(5)	−0.3184(5)	0.1669(9)	−0.0345(4)	4.5(2)
C(6)	−0.2063(5)	−0.0460(9)	0.0384(4)	4.7(2)

two types of cyanide groups in the crystal lattice. The lower frequency band corresponds to that of $K_3[M(CN)_6]$ and can be ascribed to a nonbridging cyanide group. The higher frequency band is attributed to the bridging cyanide group.[34] The intensity of the lower frequency band is stronger than that of the higher frequency band. This fact suggests a low dimensionality for the bulk structure of the assemblies.

The reflectance spectrum of **1** shows strong absorptions at 270, 277, 308, 324, and 418 nm and two weaker bands at 540 and ∼800 nm. This can be explained by the superposition of the spectra of $K_3[Fe(CN)_6]$ (with intense bands at 301, 318, and 419 nm and a weak shoulder near 500 nm) and $[Ni(en)_3]Cl_2$ (moderately intense bands at 346, 551, and 790 nm), except for the two absorptions at 270 and 276 nm. The reflectance spectrum of **2** shows well-resolved bands at 270, 276, 316, 382, 532, and ∼800 nm. This is again explained by the spectra of

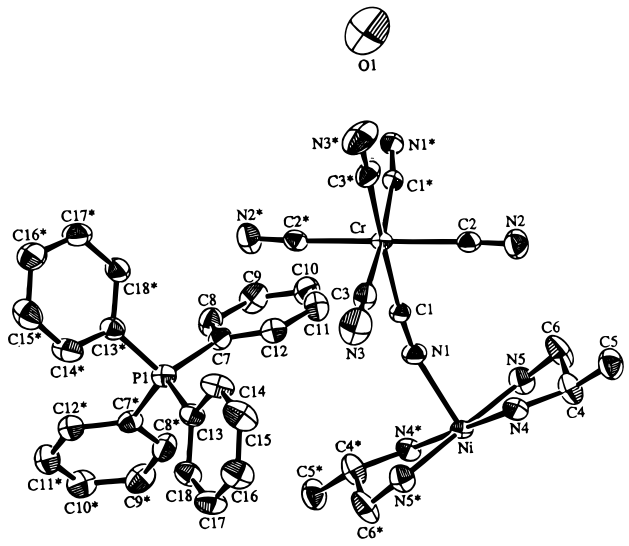

Figure 1. ORTEP drawing for the asymmetric unit of $PPh_4[Ni(pn)_2][Cr(CN)_6]\cdot H_2O$ (**2**), showing 30% probability ellipsolids.

$K_3[Cr(CN)_6]$ (intense bands at 310 and 375 nm and a weak shoulder near 465 nm) and $[Ni(en)_3]Cl_2$, except for the bands at 270 and 276 nm. The spectrum of **3** is very simplified and has two very intense bands at 270 and 277 nm, an intense band at 314 nm, and two moderately intense bands at 551 and ∼800 nm. The band at 314 nm can be assigned to the d−d transition band ($^1T_{1g} \rightarrow {}^1A_{1g}$)[41] of $[Co(CN)_6]^{3-}$ and the visible bands are assigned to the d−d transitions of the Ni(II) chromophore. The intense bands at 270 and 277 nm are commonly seen for **1**−**3** and seem to correspond to a band near 260 nm found for $K_3[M(CN)_6]$ (259 nm for M = Fe, 261 nm for M = Cr, 259 nm for M = Co). The shift of the band to a longer wavelength and the splitting into two are taken as evidence for forming the 1-D bimetallic network to be discussed below.

All the assemblies are stable in air and insoluble in most inorganic and organic solvents.

Crystal Structure. The X-ray crystallography for $PPh_4[Ni(pn)_2][Cr(CN)_6]_2\cdot H_2O$ (**2**) and $PPh_4[Ni(pn)_2][Co(CN)_6]_2\cdot H_2O$ (**3**) proves that they are isomorphous with **1**.[10] A perspective view of the asymmetric unit with the atom numbering scheme of **2** is shown in Figure 1. The projections of the molecular entity in the lattice along the *a* and *b* axes are presented in Figures 2 and 3, respectively. The selected bond distances and angles with their estimated standard deviations for **2** are listed in Table 4 together with those of **1** and **3**.

The asymmetric unit of $PPh_4[Ni(pn)_2][Cr(CN)_6]_2\cdot H_2O$ (**2**) consists of a half of a $[Cr(CN)_6]^{3-}$ anion, half of a planar $[Ni(pn)_2]^{2+}$, half of a tetraphenylphosphonium cation, and half of a water molecule. The Ni^{II} ion resides at the inversion center, and the Cr^{III} ion and P(1) atom lie on a mirror plane. Two cyano nitrogens of $[Cr(CN)_6]^{3-}$ (N(1) and N(1)* (* indicates a symmetry operation of $-x$, y, $1/2 - z$) in the cis position coordinate to the adjacent $[Ni(pn)_2]^{2+}$ cations forming a 1-D zigzag chain running along the *c* axis. (Figure 2) The intrachain Cr···Ni separation is 5.215(1) Å. The Ni−N(1) distance is 2.128(2) Å, and the C(1)−N(1)−Ni angle is 160.2(2)°. The enantiomeric *R*-pn (N4−C4(C5)−C6−N5) and *S*-pn (N4*−C4*(C5*)−C6*−N5*) coordinate to the same Ni ion, with an equatorial orientation of the methyl group (C5 and C5*). The Ni ion has a nearly octahedral surrounding showing a slight elongation along the CN−Ni−NC axis. The arrangement of

(41) Beck, W.; Feldi, K. *Z. Anorg. Chem.* **1965**, *341*, 113.

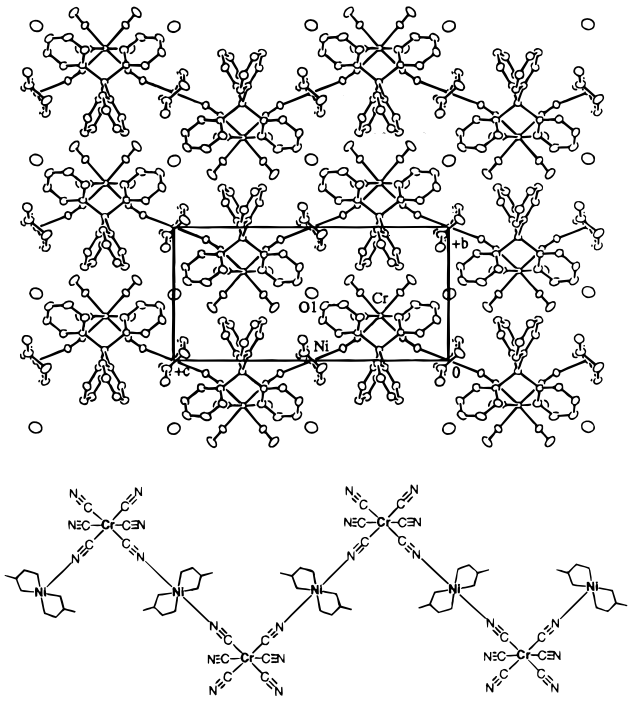

Figure 2. Projections of the network structure of **2** along the *a* axis and schematic view of the 1-D chain structure.

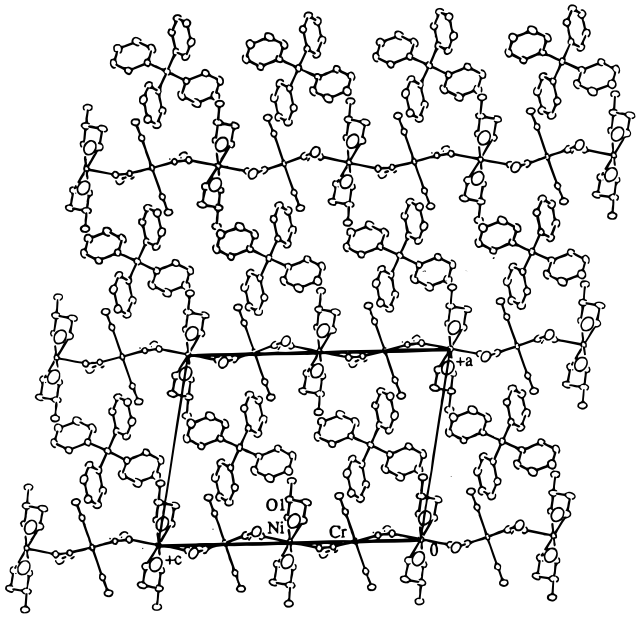

Figure 3. Projections of the network structure of **2** along the *b* axis (b).

the 1-D chains in the lattice is depicted in Figure 2. The nearest interchain metal···metal separations along the *b* axis are as follows: Cr···Cr(x, y+1, z) = Ni···Ni (x, y+1, z) = 8.454(2) Å, and Ni···Cr($-x$, $-y$+1, $-z$) = 7.149(2) Å. The corresponding interchain separations along the *a* axis are longer than 13 Å. The tetraphenylphosphonium cations and lattice water molecules are positioned between the chains.

All the bimetallic assemblies **1**−**3** have essentially the same molecular and network structures. However, they show a significant difference in the average M−C bond distance that becomes longer in the order of M = Co < Fe < Cr. This order is in accord with the decreasing number of dπ electrons at the metal center. This fact suggests that the π-back-donation from the metal to the vacant CN orbital decreases in this order (see Table 4). The *c* axis lengths of **1**−**3** reflect the M−C distance and increases in the order of M = Co < Fe < Cr (see Table 1).

Table 4. Selected Bond Distances, Separations between Metal Centers and Bond Angles of **1**, **2**, and **3**

	1 (M = Fe)	**2** (M = Cr)	**3** (M = Co)
distances (Å)			
M−C(1)	1.978(7)	2.083(3)	1.941(5)
M−C(2)	1.959(9)	2.087(3)	1.924(6)
M−C(3)	1.955(8)	2.062(3)	1.916(5)
Ni−N(1)	2.150(6)	2.128(2)	2.147(4)
intrachain separations (Å)			
Ni···M	5.116(1)	5.215(1)	5.079(1)
nearest interchain separations (Å)			
Ni···M	7.134(2)	7.149(2)	7.128(1)
Ni···Ni	8.437(3)	8.454(2)	8.437(1)
M···M	8.437(3)	8.454(2)	8.437(1)
angles (deg)			
M−C(1)−N(1)	172.6(8)	170.0(2)	172.9(5)
C(1)−N(1)−Ni	157.9(7)	160.2(2)	158.7(4)

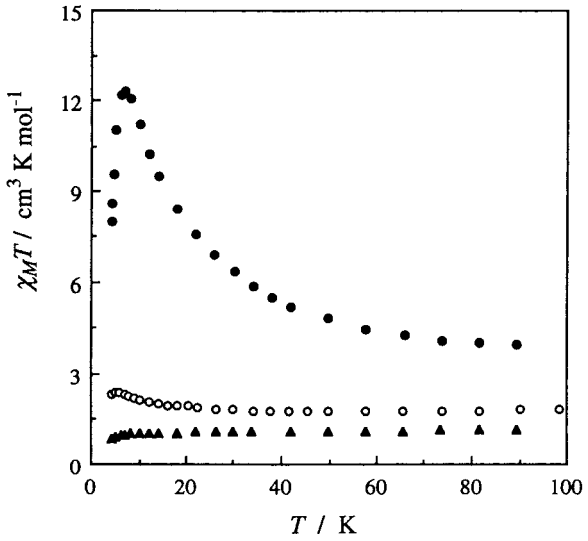

Figure 4. $\chi_M T$ *vs* T plots for $PPh_4[Ni(pn)_2][M(CN)_6]\cdot H_2O$ per NiM: M^{3+} = Fe (**1**; ○), Cr (**2**; ●), Co (**3**; ▲).

Magnetic Properties. The cryomagnetic properties of **1**−**3** have been studied in the temperature range of 4.2−300 K. The $\chi_M T$ vs T plots of **1**−**3** are given in Figure 4, where χ_M is the magnetic susceptibility per NiM unit.

Compound 1 (NiFe). The room-temperature value of $\chi_M T$ (1.94 cm^3 K mol^{-1}: 3.94 μ_B) is higher than the expected spin-only value for the noncoupled low-spin Fe^{III} and high-spin Ni^{II} ions (1.38 cm^3 K mol^{-1}: 3.32 μ_B, calculated with g = 2.0). The $\chi_M T$ value gradually decreases with temperature decreasing to the minimum value of 1.75 cm^3 K mol^{-1} (3.74 μ_B) at 50 K and then increases to the maximum value of 2.38 cm^3 K mol^{-1} (4.36 μ_B) at 5.0 K. The decrease in $\chi_M T$ from 290 to 50 K can be attributed to the orbital effect of the $^2T_2$ term of the low-spin Fe^{III} ion under pseudo O_h symmetry. The magnetic behavior below 50 K indicates the presence of a ferromagnetic exchange interaction between the low-spin Fe^{III} and Ni^{II} ions through the cyanide bridge. In accord with this, the Curie−Weiss plots in the temperature range of 5−50 K gave a positive Weiss constant of θ = +2.0 K. The ferromagnetic interaction is rationalized by the strict orthogonality of the magnetic orbitals of Fe^{III} ($(t_{2g})^1$) and Ni^{II} ($(e_g)^2$).[1,2,42] The maximum $\chi_M T$ value is common for ferromagnetically coupled Fe^{III} and Ni^{II} ions

(42) Mallah, T.; Auberger, C.; Verdaguer, M.; Veillet, P. *J. Chem. Soc., Chem. Commun.* **1995**, 61.

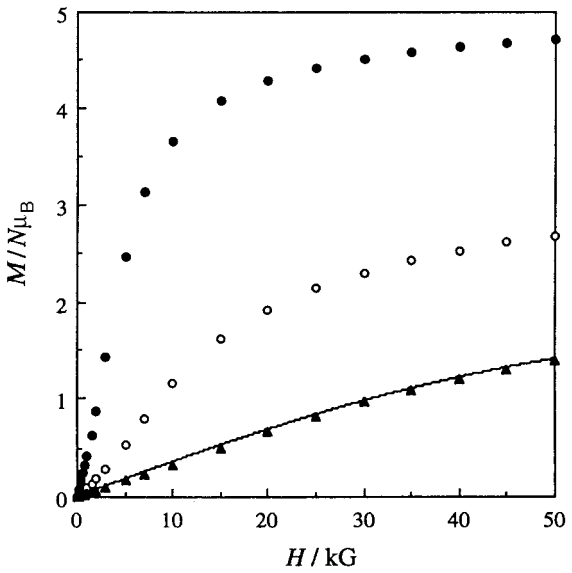

Figure 5. Field dependence of the magnetization at 5 K for $PPh_4[Ni(pn)_2][M(CN)_6]\cdot H_2O$ per NiM: M^{3+} = Fe (**1**; ○), Cr (**2**; ●), Co (**3**; ▲).

(1.88−2.48 cm^3 K mol^{-1}: 3.87−4.45 μ_B, calculated with g = 2.0−2.3). Thus, no long-range magnetic ordering occurs in this compound. Below 5.0 K, the $\chi_M T$ value tends to decrease because of a weak antiferromagnetic interchain interaction. Such an antiferromagnetic interchain interaction is not negligible for an interchain separation smaller than 10 Å.[12]

Compound 2 (CrNi). The room-temperature value of $\chi_M T$ (3.10 cm^3 K mol^{-1}: 4.98 μ_B) is slightly larger than the expected spin-only value for noncoupled Cr^{III} and Ni^{II} ions (2.88 cm^3 K mol^{-1}: 4.80 μ_B). Upon cooling, the $\chi_M T$ value gradually increases to the maximum value of 12.35 cm^3 K mol^{-1} (9.94 μ_B) at 7 K and then decreases down to 8.01 cm^3 K mol^{-1} (8.00 μ_B) at 4.2 K. The decrease in $\chi_M T$ below 7 K is probably due to an antiferromagnetic interchain interaction. The magnetic behavior in the range of 7−290 K indicates the presence of a ferromagnetic exchange interaction between the Cr^{III} and Ni^{II} ions through the cyanide bridge.[1,2] The Curie−Weiss plot (7−90 K) forms a straight line with a positive Weiss constant of θ = +9.8 K. It must be noted that the maximum $\chi_M T$ value is significantly larger than the spin-only value for ferromagnetically coupled Cr^{III} and Ni^{II} ions (4.38 cm^3 K mol^{-1}: 5.92 μ_B). This fact suggests a magnetic ordering tendency in the chain, though no remnant magnetization is observed at 4.2 K. It is likely that the magnetic ordering over the lattice is overcome by the antiferromagnetic interchain interaction.

Compound 3 (CoNi). The $\chi_M T$ value at 290 K is 1.08 cm^3 K mol^{-1} (2.94 μ_B) that is in good agreement with the spin-only value of 1.00 cm^3 K mol^{-1} (2.83 μ_B) for Ni^{II}. No magnetic interaction is presumed within the chain because of the diamagnetic nature of Co^{III}. The $\chi_M T$ vs T plot shows a slight decrease with the decrease in temperature to 0.85 cm^3 K mol^{-1} (2.61 μ_B) at 4.3 K. This may be attributed to a weak antiferromagnetic interchain interaction. The $1/\chi_M$ vs T plot in the range of 4.3−290 K obeys the Curie−Weiss law with a negative Weiss constant of θ = −1.3 K.

The field dependences of the magnetization M for **1**−**3** up to 50 kG were measured at 5.0 K, and the curves are shown in Figure 5. The magnetization curve of **3** is well simulated by the theoretical equation $M = g\mu_B SNB_s(x)$ with S = 2/2, where N, μ_B, and $B_s(x)$ are Avogadro's number, the Bohr magneton, and the Brillouin function, respectively. Compounds **1** and **2** showed maximum magnetization values of 2.69 and 4.70 $N\mu_B$, respectively. These values are respectively close to the expected saturation value of 3 $N\mu_B$ ($S = {}^1/_2 + {}^2/_2$) for **1** and 5 $N\mu_B$ ($S = {}^3/_2 + {}^2/_2$) for **2**, which indicate a ferromagnetic coupling between the M^{III} and Ni^{II} ions, while the slopes of the curve for **1** and **2** slightly increased above ca. 1.5 kG. Such an inflection is not observed in the curve for **3**. These results suggest that chains are antiferromagnetically coupled in the lattice and the antiferromagnetic interchain interaction of **1** and **2** are stronger than that of **3**.

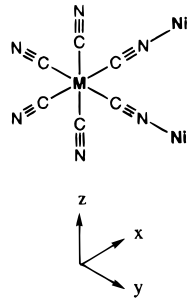

Figure 6. Schematic representation of the dπ magnetic orbitals for (a) d_{xy} and (b) d_{xz} (d_{yz}) unpaired electron of $[M(CN)_6]^{3-}$.

Chart 1

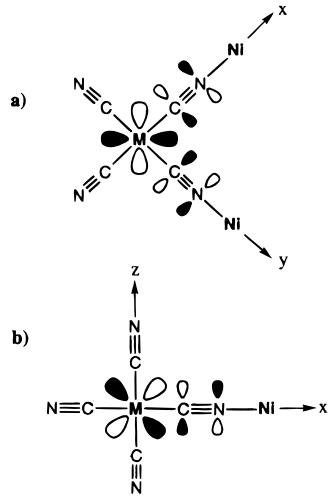

Based on the Weiss constant determined from the Curie Weiss plot, **2** (θ = +9.8 K) shows a strong ferromagnetic interaction compared with **1** (θ = +2.0 K). The relative strength of the ferromagnetic interaction cannot be interpreted in the M···Ni intermetallic separation in the chain since the Cr···Ni separation (5.215(1) Å) of **2** is larger than the Fe···Ni separation of **1** (5.116(1) Å). It appears that the electronic configuration of the M^{III} ion is concerned with the different magnetic nature between **1** and **2**. It must be noted that the $[M(CN)_6]^{3-}$ entity in **1** and **2** has the local symmetry of C_{2v}. When the x, y, and z axes are taken as depicted in Figure 6, the orbitals of dπ character are separated into two sets of (d_{xy}) and (d_{xz}, d_{yz}); the d_{xz} and d_{yz} orbitals belong to different irreducible representations of the group C_{2v}, but they are energetically degenerate. Thus, the magnetic orbital of the $[Fe(CN)_6]^{3-}$ in **1** is depicted by either $(d_{xy})^1$ or $(d_{xz}, d_{yz})^1$, which can be concerned with the dπ−pπ interaction as schematically shown by (a) or (b) in Chart 1 respectively. Based on the polarized neutron diffraction study for $[Fe(CN)_6]^{3-}$ and $[Cr(CN)_6]^{3-}$, the dπ−pπ interaction produces a large spin density on the pπ orbital of the cyanide nitrogen.[43−46] We presume that the interaction mechanism (a) is more efficient than (b) in spin-polarization on the cyanide nitrogen. Based on this presumption and taking into account

the weak ferromagnetic interaction in **1** relative to **2**, the magnetic orbital of Fe^{III} in **1** is deduced $(d_{xz}, d_{yz})^1$. The fact that the Fe−C(1) bond is elongated relative to the Fe−C(2) and Fe−C(3) bonds implies a decrease in the π-back-donation from the iron d_{xy} orbital to the vacant CN^- orbital and destabilization of the d_{xy} orbital.

In the case of **2**, the Cr^{III} under C_{2v} symmetry has three unpaired electrons on the d_{xy}, d_{xz}, and d_{yz} orbitals so that mechanisms (a) and (b) (Chart 1) operate together, giving rise to a strong ferromagnetic interaction between the nearest Cr^{III} and Ni^{II} ions in the chain.

The $\chi_M T$ vs T plots for **1**−**3** (Figure 4) indicate an antiferromagnetic interchain interaction. In the case of **3**, the interchain interaction occurs between the Ni^{II} ions because the Co^{III} ion is diamagnetic. A small drop in $\chi_M T$ of **3** near the liquid helium temperature means a very weak antiferromagnetic interaction between Ni^{II} ions in the nearest interchain separation of 8.437(1) Å along the *b* axis. The metal ion pair in the nearest interchain separation is Ni···M along the *b* axis (Ni···Fe, 7.134(2) Å; Ni···Cr, 7.149(2) Å; Ni···Co, 7.128(1) Å) that may have a dominant contribution to the interchain antiferromagnetic interaction in **1** and **2**. This interpretation is consistent with the results of the *M vs H* curve.

Thus, **2** shows a fairly strong ferromagnetic interaction between the adjacent Cr^{III} and Ni^{II} ions within the 1-D chain, but a significant antiferromagnetic interaction occurs between the chains to cancel the spins accumulated within the 1-D chain. As the result of the two competitive effects, no spontaneous magnetization occurs despite reaching a large maximum $\chi_M T$ value near the liquid helium temperature.

(43) Figgis, B. N.; Forsyth, J. B.; Mason, R.; Reynords, P. A. *Chem. Phys. Lett.* **1985**, *115*, 454.
(44) Figgis, B. N.; Forsyth, J. B.; Reynords, P. A. *Inorg. Chem.* **1987**, *26*, 101.
(45) Figgis, B. N.; Kucharski, E. D.; Virtis, M. *J. Am. Chem. Soc.* **1993**, *115*, 176.
(46) Daul, C. A.; Day, P.; Figgis, B. N.; Gudel, H. U.; Herren, F.; Ludi, A.; Reynords, P. A. *Proc. R. Soc. London* **1988**, *A419*, 205.

Conclusion

The reaction of $[Ni(pn)_3]Cl_2$, $K_3[M(CN)_6]$ and PPh_4Cl in the 1:1:1 molar ratio in aqueous solution formed bimetallic assemblies of $PPh_4[Ni(pn)_2][M(CN)_6]\cdot H_2O$ (M^{III} = Fe (**1**), Cr (**2**), Co (**3**)). They have a 1-D zigzag chain structure constructed of the alternate array of $[M(CN)_6]^{3-}$ and the planar $[Ni(pn)_2]^{2+}$. Compound **1** shows a ferromagnetic intrachain interaction based on the strict orthogonality between the magnetic orbitals of Fe^{III} and Ni^{II}. No magnetic ordering occurs in this compound because of the antiferromagnetic interchain interaction. Compound **2** also shows a ferromagnetic interaction between the adjacent Cr^{III} and Ni^{II} ions within the chain. A tendency of magnetic ordering over the lattice is observed which, however, is overcome by the interchain antiferromagnetic interaction, providing an antiferromagnet over the lattice. Compound **3** is essentially paramagnetic within the 1-D chain, showing a weak antiferromagnetic interchain interaction.

The $[M(CN)_6]^{3-}$ in the assemblies has the local symmetry C_{2v} with the d orbital order of $d_{xy} > d_{xz}, d_{yz}$ (*x* and *y* axes are taken along the M−CN−Ni bridges) and an efficient ferromagnetic interaction in the M^{III}−CN−Ni^{II} unit occurs when the M^{III} ion has an unoccupied electron on the d_{xy} orbital (i.e. **1** < **2**).

Acknowledgment. The authors thank Prof. Hiizu Iwamura and Dr. Kenji Matsuda (Institute for Fundamental Research of Organic Chemistry, Kyushu University) for their help in the magnetization measurements. This work was supported by a Grant-in-Aid for Scientific Research (No. 09740494) from the Ministry of Education, Science and Culture, Japan.

Supporting Information Available: Details pertaining to crystallographic structure determination and tables of magnetic susceptibility and magnetization of **1**, **2**, and **3** are available (51 pages). Three X-ray crystallographic files, in CIF format, are also available on the Internet only. Ordering and access information is given on any current masthead page.

IC9704748